ORIGINAL PAPER

Interleukin-22 promotes tumor angiogenesis

Nicholas J. Protopsaltis[1] · Wei Liang[1] · Eric Nudleman[2] · Napoleone Ferrara[1]

Abstract

$T_H 17$ cells play important yet complex roles in cancer development and progression. We previously reported that $T_H 17$ cells and IL-17 mediate resistance to anti-VEGF therapy by inducing recruitment of immunosuppressive and proangiogenic myeloid cells to the tumor microenvironment. Here, we demonstrate that IL-22, a key effector cytokine expressed by $T_H 17$ cells, directly acts on endothelial cells to promote tumor angiogenesis. IL-22 induces endothelial cell proliferation, survival, and chemotaxis in vitro and neovascularization in an ex vivo mouse choroid explant model. Blockade of IL-22, with a neutralizing antibody, significantly inhibits tumor growth associated with reduced microvascular density. No synergistic effect of IL-22 with VEGF was observed. These results identify IL-22 as a potential therapeutic target for blocking tumor angiogenesis.

Keywords Inflammation · Angiogenesis · Tumor · Cytokine

Introduction

Angiogenesis plays an essential role in many physiologic and pathological conditions. Identification of proangiogenic factors, such as VEGF, has led to the development of effective therapeutics in oncology and ophthalmology. VEGF is upregulated in most tumors, and anti-VEGF therapy has been approved for the treatment of several malignancies including in metastatic colorectal carcinoma, metastatic renal cell carcinoma, non-small cell lung cancer, glioblastoma multiforme, and ovarian cancer [1]. However, similar to other oncological therapies, some patients eventually develop refractory disease and resistance to anti-VEGF treatment, suggesting the existence of VEGF-independent mechanisms and warranting the identification of additional proangiogenic pathways [2].

It is increasingly recognized that the tumor angiogenesis is determined not only by endothelial cells but also by the crosstalk between endothelial cells and other cell types in the tumor microenvironment [3–5]. Work from several laboratories has shown that stromal cells, such as myeloid cells and fibroblasts, can promote tumor angiogenesis through expression of various proangiogenic factors, including Bv8/PROK2, members of the PDGF, FGF, VEGF and angiopoietin families [6–14].

Although all types of immune cells can be found in a tumor, their distribution and significance varies among different tumor types [15]. The CD4+ T helper type 17 cell ($T_H 17$) is a relatively newly discovered subtype of adaptive immune cells, and specializes in removing extracellular bacteria and fungi [16]. Although implicated in a number of diseases, $T_H 17$ cells are increasingly being recognized as a major component of infiltrating tumor lymphocytes, and among different types of immune cells, are particularly varied in whether they promote or inhibit tumor progression [15, 17]. Recently, we reported that IL-17, secreted by $T_H 17$ cells, can mediate resistance to anti-VEGF treatment through induction of G-CSF expression and thus promoting recruitment of proangiogenic myeloid cells [11]. However, whether $T_H 17$ cells have direct impact on endothelial cells remains unclear. In this study, we investigated the effects of IL-22, another key effector cytokine expressed by $T_H 17$ cells, on endothelial cell functions and tumor angiogenesis. IL-22 is a tightly regulated pro-inflammatory member of the IL-10 family that signals through the IL-22 receptor, composed of a ubiquitous IL-10R2 subunit and a restrictively expressed

✉ Napoleone Ferrara
nferrara@ucsd.edu

1 Moores Cancer Center, University of California San Diego, La Jolla, CA 92093, USA

2 Shiley Eye Institute, University of California San Diego, La Jolla, CA, USA

IL-22R1 subunit [18, 19]. The physiologic role of IL-22 is to promote would healing and tissue repair, but uniquely among immune cell-derived cytokines, IL-22 only acts on non-hematopoietic cells. Thus, while IL-22 is thought to have a protective effect on the epithelium, IL-22 levels correlate with chemo-resistance in patients with colorectal carcinoma [20]. Further evidence for pro-tumor effects of IL-22 was provided in a mouse model, where IL-22 promoted colonic inflammation and maintenance of colorectal carcinoma [21]. IL-22 is not only implicated in colorectal carcinoma, but has also been found to be elevated in gastric, hepatocellular, large- and small-cell lung carcinomas [22]. Our work on the function of IL-22 in tumor angiogenesis can provide further insights in how TH17 cells promote cancer development and progression, and rationales for developing new therapies against tumor angiogenesis.

Results

Expression of IL-22 receptor in endothelial cells

To determine expression of IL-22 receptor in endothelial cells, we first performed Western blot analyses to show that IL-22 receptor is expressed in human umbilical vein endothelial cells (HUVEC) and microvascular endothelial cells (HMVEC) (Fig. 1a). HepG2 cells that are known to express IL-22 receptor were used as a positive control (Fig. 1a). Next, we performed flow cytometry analyses to measure expression levels of IL-22 receptor on the cell surface. Similar to HepG2 cells, both HUVECs and HMVECs demonstrate increased mean fluorescence intensity with IL-22 receptor antibody staining, compared to
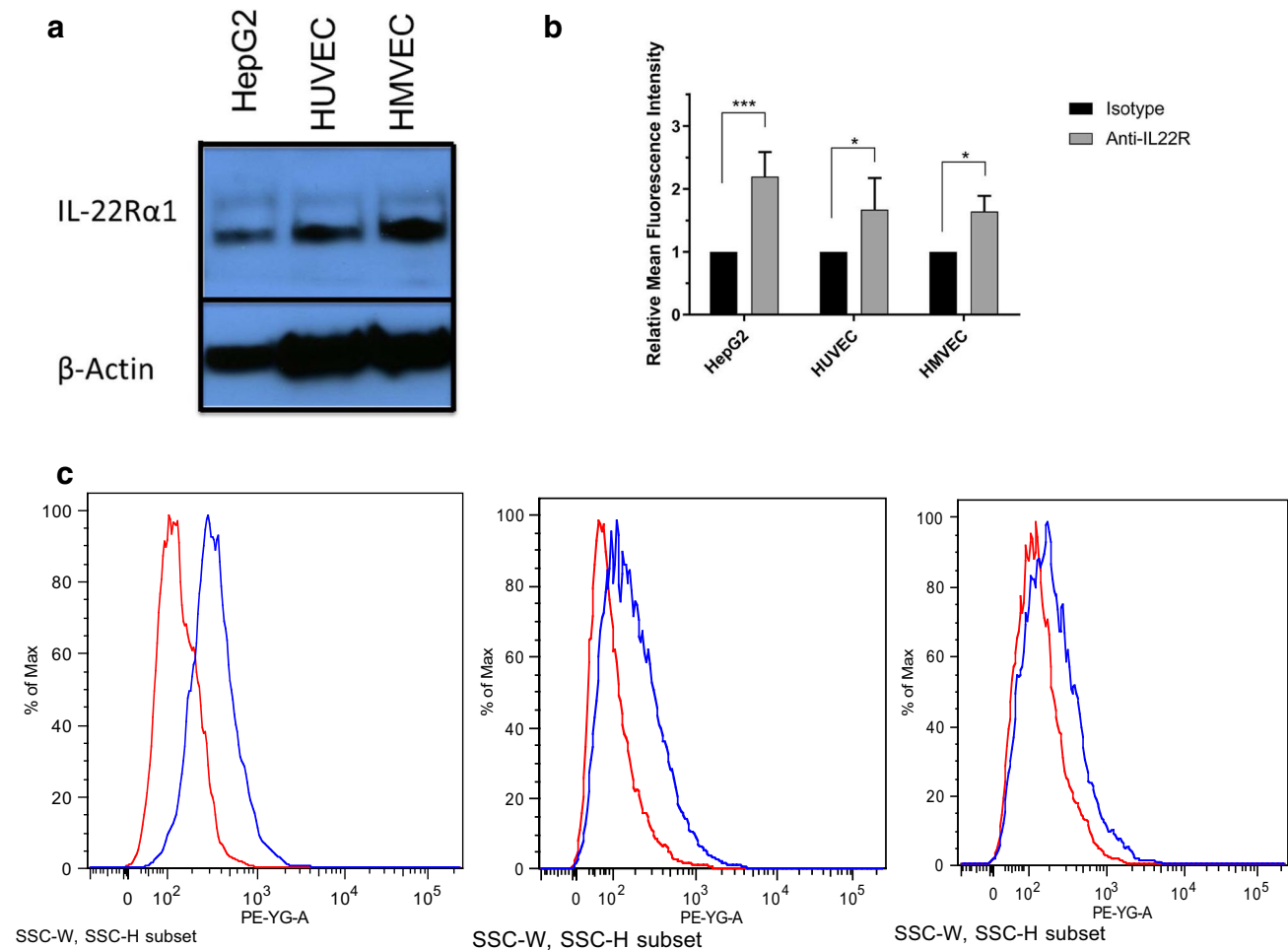

Fig. 1 Expression of IL-22 Receptor in endothelial cells. **a** Western blot analyses of expression of IL-22 receptor in HepG2, HUVEC and HMVEC cells. β-actin was used as control for equal loading. **b** Quantification of surface expression levels of IL-22 receptor by flow cytometry. Mean fluorescence intensity of staining with anti-IL-22R or isotype IgG was calculated. Results are expressed as fold changes between anti-IL22R and isotype IgG (set to 1). Error bars indicate standard deviation, $N=3$ independent experiments, ***$p<0.001$, *$p<0.05$. **c** Representative histogram of staining with anti-IL-22R (blue) or isotype IgG (red) (left: HepG2; middle: HUVEC; right: HMVEC)

isotype control (Fig. 1b, c). Together, these results suggest that IL-22 receptor is expressed in endothelial cells and accessible to extracellular ligand stimulation.

IL-22 promotes endothelial cell proliferation, survival, and migration

Endothelial cells are among the most quiescent cells in the human body, with steady state proliferation rates approaching zero. However, with appropriate stimulation, in the setting of inflammation or injury, they can re-enter the cell cycle [23]. Treatment with IL-22 stimulated HUVEC and HMVEC cell proliferation and survival, in a dose-dependent manner (Fig. 2a–d). To determine the effects of IL-22 on endothelial cell chemotaxis, Boyden chamber assays were performed as previously described [24]. Compared to PBS, IL-22 can significantly stimulate HUVEC and HMVEC cell migration (Fig. 2e, f). Together, these results suggest that IL-22 can directly stimulate endothelial cell proliferation, survival and migration.

To characterize the downstream signaling pathways elicited by IL-22 in endothelial cells, we performed Western blot analyses and found that incubation with IL-22 for 30 min resulted in increased phosphorylation of ERK1/2 and Stat3 in HUVECs (Fig. 3a) and HMVECs (Fig. 3b). Quantification of the relative change in the expression demonstrated statistically significant increases (Fig. 3c, d).
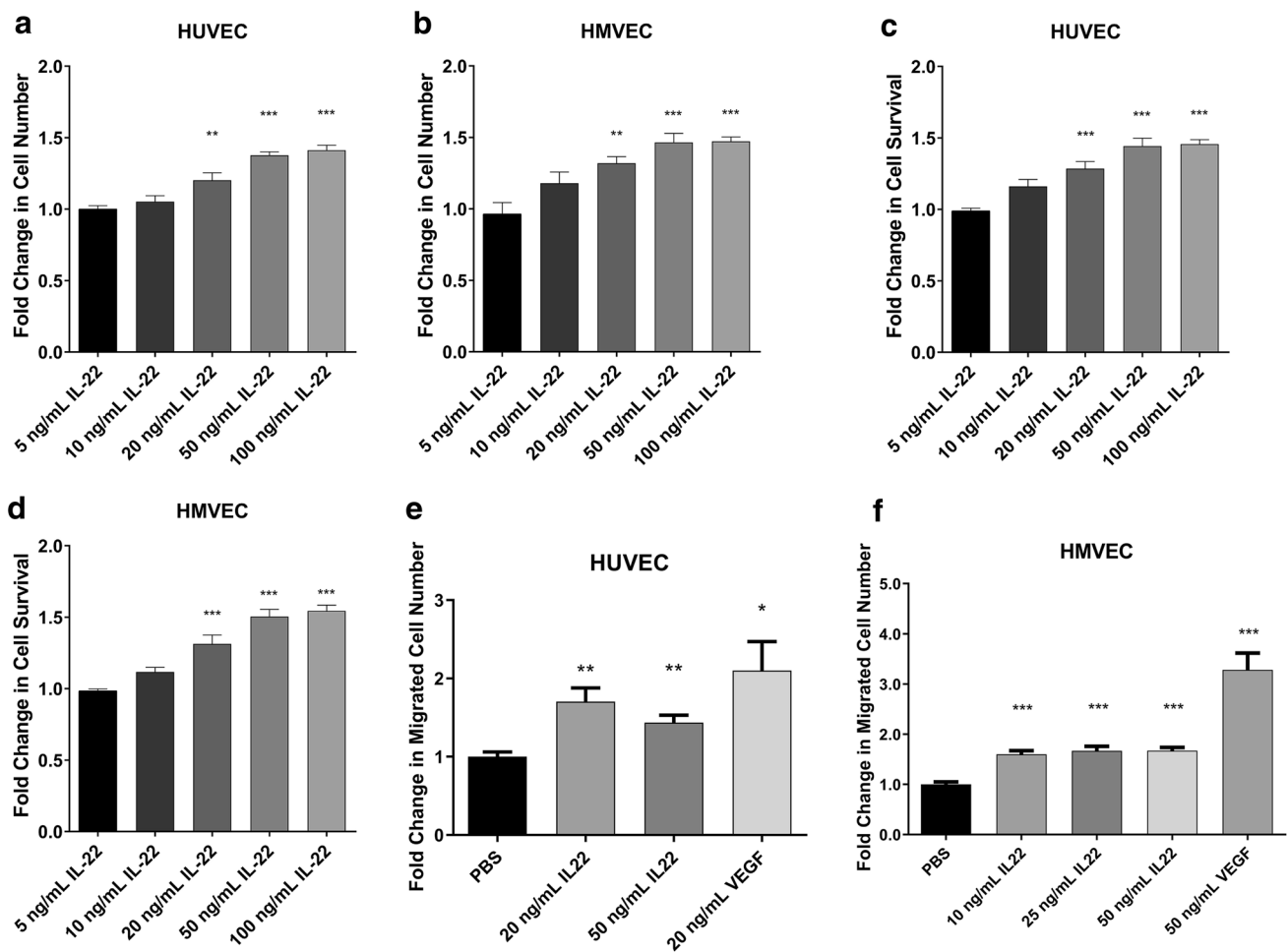

Fig. 2 IL-22 Promotes Endothelial Cell Proliferation, Survival and Migration. **a, b** HUVECs or HMVECs were treated with indicated concentrations of IL-22 for 3 days or 6 days, respectively. Cell numbers were determined and the results are expressed as fold increase of cell numbers above control (set to 1). Error bars indicate standard error of the mean. **p < 0.01, ***p < 0.001, N = 4 experiments. **c, d** HUVECs or HMVECs were treated with indicated concentrations of IL-22 for 3 days or 6 days, respectively. Cell survival was determined by the Cell Viability/Cytotoxicity assay and the results are expressed as fold increase above control (set to 1). Error bars indicate standard error of the mean. **p < 0.01, ***p < 0.001, N = 4–5 experiments with 2–4 replicates each. **e, f** HUVEC and HMVEC cell migration in response to indicated concentrations of cytokines was assessed by the Boyden chamber assay (n = 8–18 replicates from 4 pooled experiments). Results are expressed as fold changes in migrated cell numbers above control (set to 1). *p < 0.05, **p < 0.01, ***p < 0.001

a

HUVEC

0 5 10 20 50 100   ng/ml IL-22

p-Stat3

Stat3

p-ERK1/2

ERK1/2

β-actin

b

HMVEC

0 5 10 20 50 100   ng/ml IL-22

p-Stat3

Stat3

p-ERK1/2

ERK1/2

β-actin

c

p-ERK1/2

Fold increase above control

5 10 20 50 100   ng/ml IL-22

HUVEC   HMVEC

d

p-Stat3

Fold increase above control

5 10 20 50 100   ng/ml IL-22
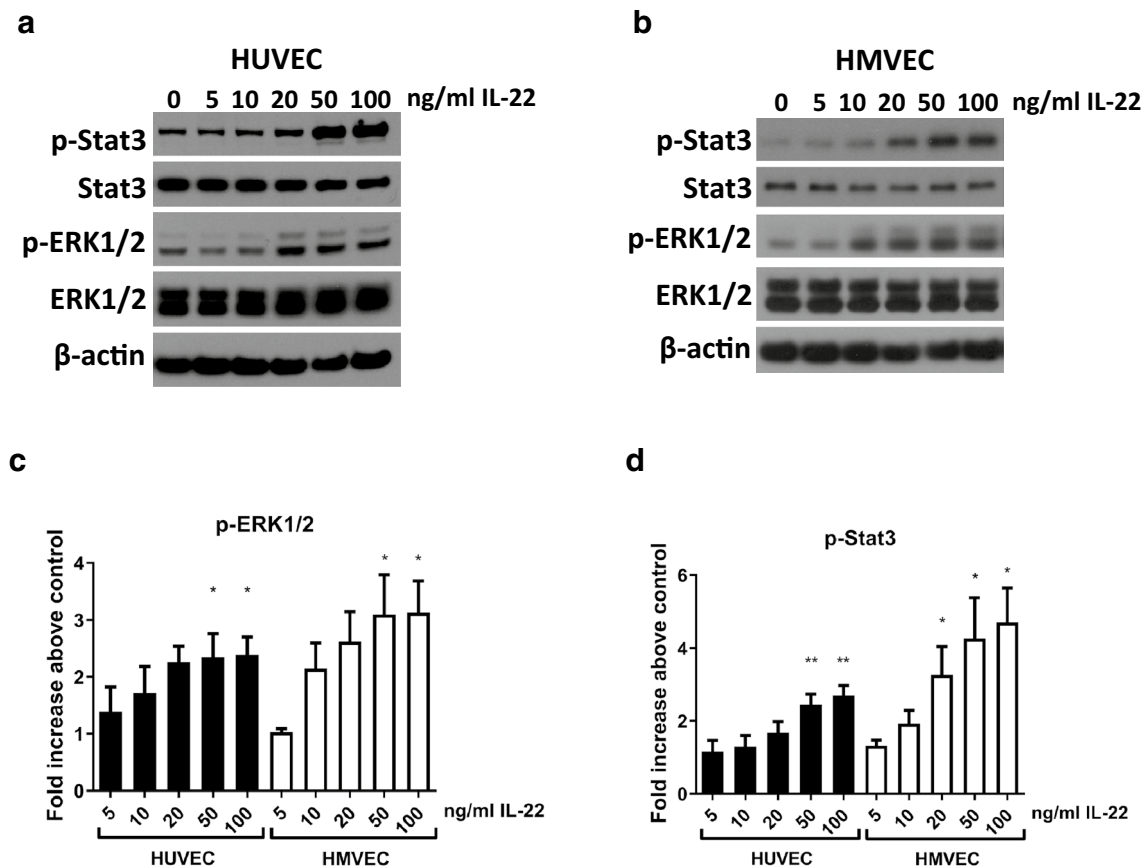
HUVEC   HMVEC

Fig. 3 IL-22 stimulates phosphorylation of ERK1/2 and Stat3. HUVECs (**a**) or HMVECs (**b**) were serum-starved and stimulated with indicated concentrations of IL-22 for 30 min. Representative western blot results of phosphorylated and total proteins are presented, with β-actin used as control for equal loading. Western Blot results were quantified as described in the "Methods" and data are expressed as fold increase of normalized protein phosphorylation by IL-22 treatment, compared to control (onefold) (**c, d**) ($N=3$), $*p < 0.05$, $**p < 0.01$

IL-22 stimulates choroidal vessel outgrowth

Explanted choroidal tissues embedded in Matrigel can serve as an ex vivo model for studying microvascular angiogenesis [24, 25]. We found that IL-22 at 5, 10, and 25 ng/mL promoted vessel outgrowth from mouse choroidal tissues (Fig. 4), an effect that is comparable to VEGF stimulation and significantly greater than control.

Blockade of IL-22 inhibits tumor growth and angiogenesis

As noted above, we documented proangiogenic effects of IL-22 in in vitro and ex vivo models. Next, we sought to determine whether IL-22 plays a role in tumor angiogenesis, using mouse tumor models. We selected EL4 mouse T-cell lymphoma and GL261 mouse glioblastoma cell lines, since these tumor cells minimally express the IL-22 receptor and do not respond to IL-22 treatment in culture (Fig. 5).

EL4 tumors are highly aggressive and have been previously shown to be resistant to anti-VEGF therapy owing to the ability to recruit myeloid cells of the neutrophil lineage [11, 26]. IL-22 was released by EL4 cells into the conditioned medium and such release was significantly enhanced by hypoxia in the presence of TGF-β and IL-6 two cytokines previously reported to stimulate IL-22 released from Th17 cells [27] (Supplementary Fig. 1). We were not able to detect IL-22 in GL261 cell conditioned medium under normoxic or hypoxic conditions (data not shown), despite the fact that IL-22 protein could be detected in primary GL261 tumors in vivo. However, we cannot rule out the possibility that GL261 may produce IL-22 in response to specific stimuli. In this context, IL-22 was not found to be constitutively produced by freshly isolated splenocytes, but was detectable following stimulation with Concanavalin A [28].

Next, we investigated whether blockade of IL-22 using a neutralizing antibody affects tumor growth and angiogenesis. First, we confirmed that anti-IL-22 antibody did
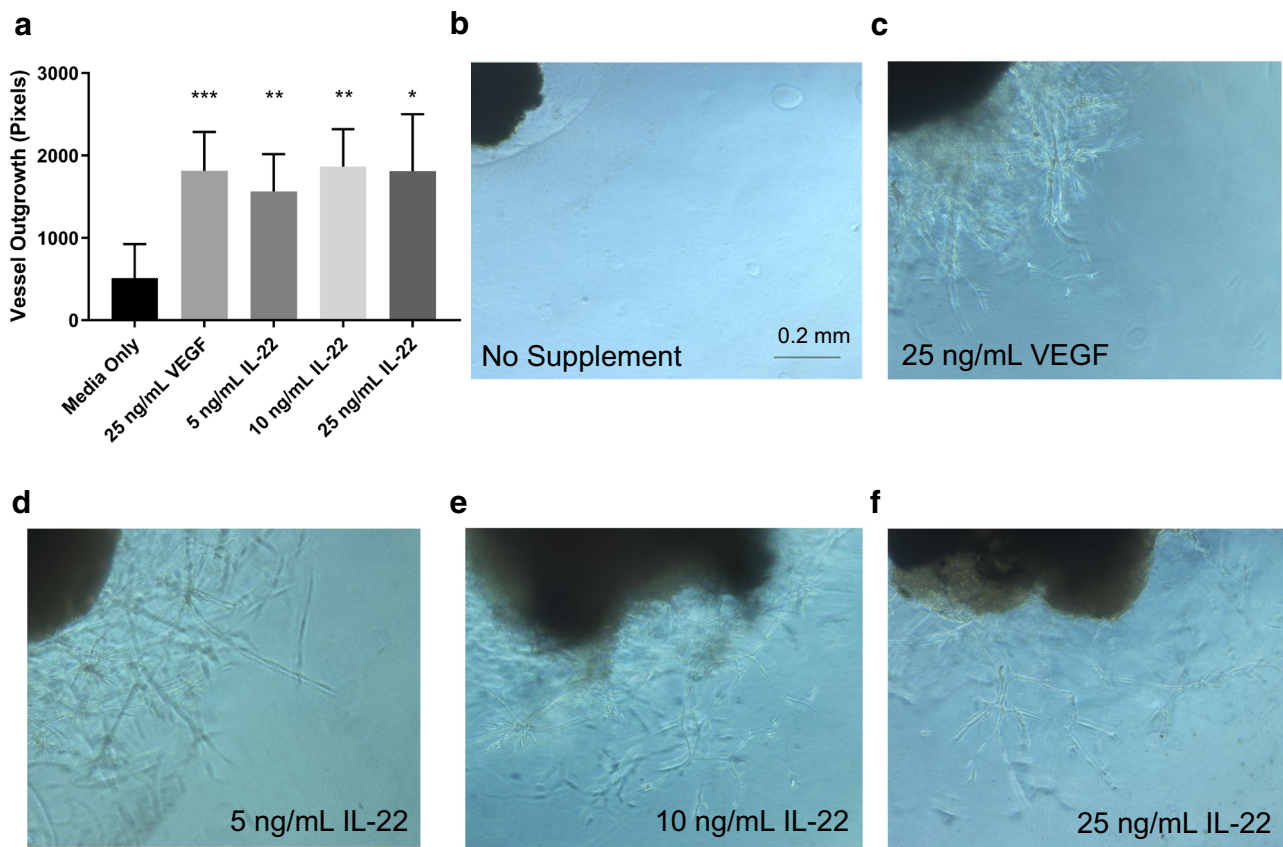
Fig. 4 IL-22 induces Vessel outgrowth in a mouse choroid explant model. **a** Quantification of vessel outgrowth ($N = 3$ experiments, total number of 6–10 replicates per experimental condition). **b–f** Repre-sentative images of vessel growth after 6 day incubation. *$p < 0.05$, **$p < 0.01$, ***$p < 0.001$

not inhibit tumor cell growth in culture, compared to an IgG1A control antibody (Supplementary Fig. 2). Intraperitoneal administration of anti-IL22 antibody resulted in a dose-dependent reduction of EL4 tumor growth compared to isotype control (Fig. 6a). Given that both IL-22 and VEGF had growth-promoting effects on endothelial cells in-vitro, we postulated that IL-22 and VEGF might be acting additively or synergistically to enhance tumor angiogenesis and growth in vivo. To address this possibility, anti-IL-22 and anti-VEGF were given to EL4 tumor-bearing mice, alone or in combination. However, compared to anti-IL-22 or anti-VEGF monotherapy, the combination did not further inhibit tumor growth (Fig. 6b).

We also utilized Rag1$^{-/-}$ mice that lack mature T or B cells and found that anti-IL22 significantly inhibited tumor growth (Fig. 6c). Analysis of EL4 tumors collected from Rag1$^{-/-}$ mice revealed that the mice treated with anti-IL22 or anti-VEGF antibody had a statistically significant decrease in tumor weight compared to those treated with isotype control (Fig. 6d). Staining for the endothelial cell marker CD31 in the tumors from Rag1$^{-/-}$ mice indicated a significant decrease of CD31+ area by anti-IL22 or anti-VEGF, compared to control (Fig. 6e).

We also examined the effects of anti-IL-22 treatment on GL261 tumor growth in C57BL/6 mice. Administration of anti-IL-22 or anti-VEGF antibody resulted in a statistically significant decrease in tumor growth compared to isotype control (Fig. 7a). ELISA analysis revealed an increase of intra-tumor IL-22 in the mice treated with anti-VEGF anti-body (Fig. 7b). In athymic nude mice, both anti-IL22 and anti-VEGF monotherapy resulted in a significant reduction in tumor growth compared to isotype control treatment (Fig. 7c). ELISA analysis revealed that the mice treated with anti-VEGF monotherapy had higher tumor concentrations of IL-22 compared to those treated with isotype control (Fig. 7d). CD31 staining on GL261 tumors from C57BL/6 mice revealed no difference between control and anti-IL-22-treated groups (data not shown).
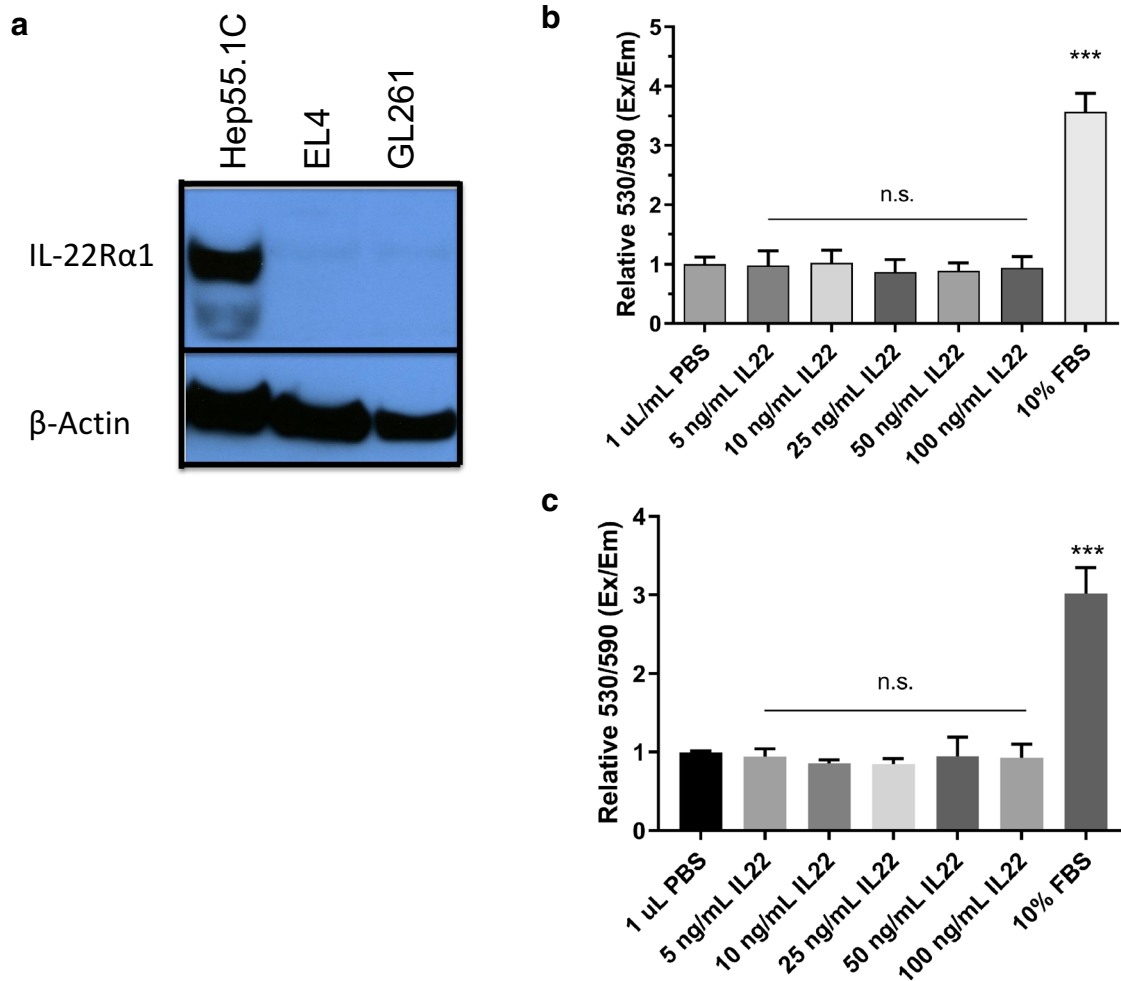
Fig. 5 Lack of expression of IL-22 receptor and mitogenic response to IL-22 in EL4 and Gl261 cells. **a** Representative Western blot results of expression of IL-22 receptor. β-actin was used as control for equal loading. **b, c** IL-22 stimulation does not increase proliferation of EL4 (**b**) or GL261 cells (**c**). $n = 6$–11 replicates from three independent experiments. *n.s.* not significant, ***$p < 0.001$

Discussion

IL-22 is a proinflammatory cytokine expressed by T_H17 cells and plays key roles in multiple inflammatory diseases [19]. Previously, we reported that T_H17 cells mediate anti-VEGF resistance in tumors through an IL-17 paracrine network [11]. IL-22R was known to be expressed by epithelial cells of the digestive organ, respiratory tract, and skin [22]. Here, we observed that human endothelial cells express IL-22R, suggesting that like IL-17, IL-22 may play a role in angiogenesis. Further support of this notion was recently provided by He et al., who reported that treating HUVECs with IL-22 caused an increase in proliferation, and Wu et al. who observed a pro-survival effect of IL-22 on pulmonary microvascular cells in a model of lung injury [29, 30]. We observed similar effects by IL-22 under high and low serum concentrations, respectively. In addition, Shang et al. reported that endometrial stromal cells may produce IL-22 in the setting of adenomyosis, which could stimulate and cross talk with endothelial cells in vitro [31]. However, these studies did not provide evidence that IL-22 induces angiogenesis in vivo, and this is to the best of our knowledge the first report showing that IL-22 is involved in tumor angiogenesis in vivo.

It was previous reported that IL-22 can activate Stat3 and ERK in a hepatoma cell line, and later studies revealed that IL-22 induces Stat3 activation in keratinocytes and endothelial cells [30, 32, 33]. Consistently, we identify ERK and Stat3 as downstream signaling molecules for IL-22 in endothelial cells.

We found that hypoxia, a common feature in solid tumors, can increase IL-22 expression in EL4 tumor cells. This is likely mediated by HIF-1α, as previously reported [34]. Indeed, inhibition of tumor angiogenesis by anti-VEGF
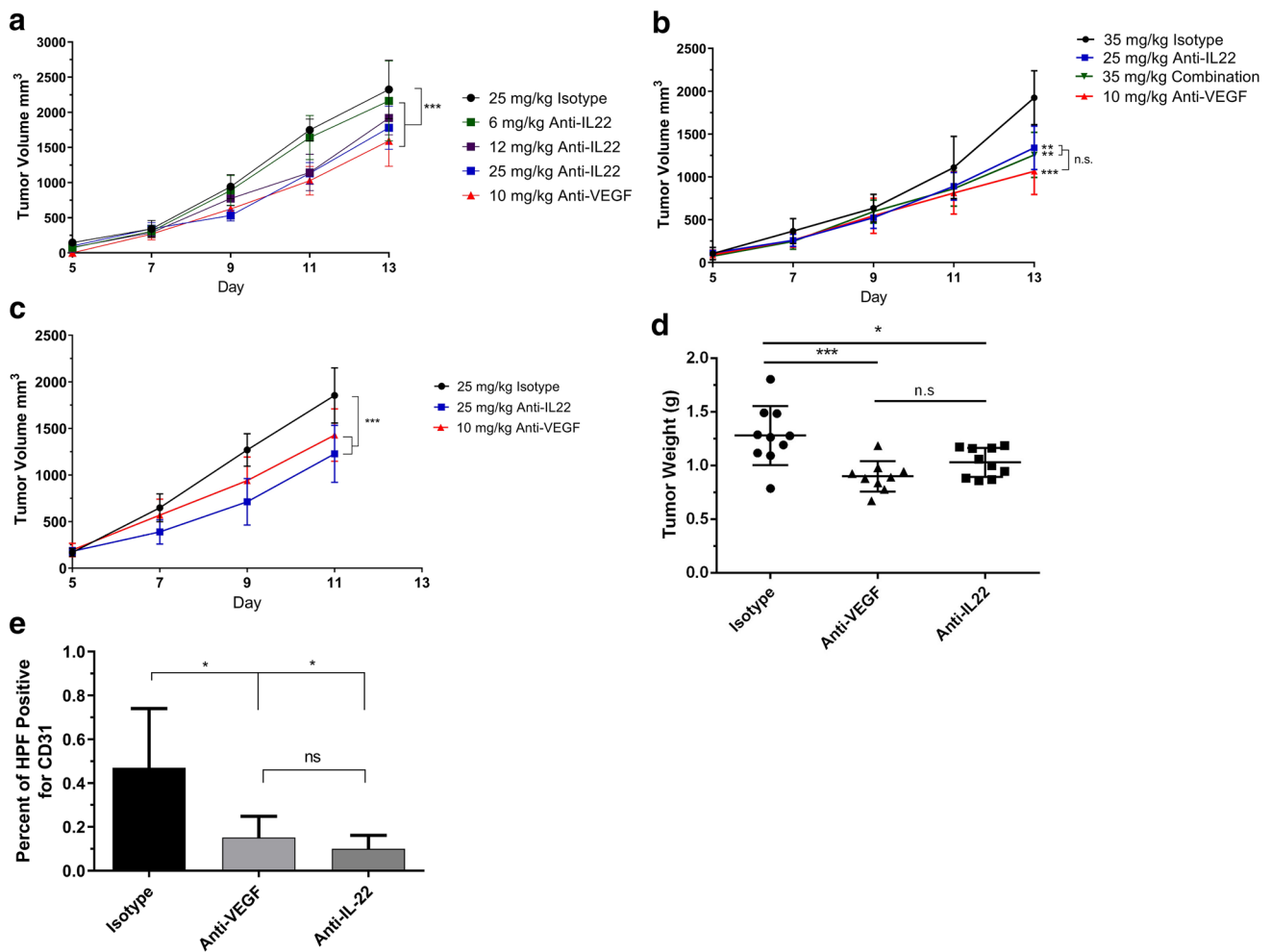
Fig. 6 Effects of anti-IL22 on EL4 tumor growth. **a, b** EL4 Tumor volume in C57BL/6 mice ($n=5$ for a, $n=8$ for b). **c** EL4 tumor volume in Rag1$^{-/-}$ mice ($n=9$–10), **d** EL4 tumor weight in Rag1$^{-/-}$ mice ($n=9$–10). **e** Quantification of CD31+ microvessel density in EL4 tumors from Rag1$^{-/-}$ mice ($n=5$). Error bars indicate standard deviation. *n.s.* not significant, $*p < 0.05$, $**p < 0.01$, $***p < 0.001$

treatment leads to increased IL-22 levels in the tumor microenvironment, which suggests IL-22 can provide an alternative angiogenic pathway in the setting of hypoxia.

Our previous work showed that IL-17, expressed by T$_H$17 cells, can induce G-CSF expression and thus facilitate recruitment of immunosuppressive and proangiogenic myeloid cells [11]. In that study, combined blockade of IL-17 and VEGF inhibited tumor growth that was otherwise resistant to anti-VEGF. Here, we tested IL-22 in a similar setting and found that the combination of anti-IL-22 and anti-VEGF did not further enhance the anti-tumor efficacy of either anti-VEGF or anti-IL-22. These results suggest that, although IL-22 alone can promote tumor angiogenesis, resistance to anti-VEGF therapy does not appear to be mediated by IL-22, at least in the models that we examined. Furthermore, despite finding both of the T$_H$17 cell cytokines IL-17 and IL-22 can induce angiogenesis and promote tumor growth, our experimental results indicate that they may have

different targets and functions within the tumor microenvironment. While IL-17 acts primarily on tumor-associated fibroblasts to mediate VEGF-independent tumorigenesis, IL-22 appears to act directly on endothelial cells to induce tumor angiogenesis. While our results from the EL4 model suggests a direct inhibition of anti-IL-22 on tumor angiogenesis, other nonendothelial-related mechanisms cannot be excluded and may contribute to the antitumor effects of anti-IL-22. For example, IL-22 synergizes with tumor necrosis factor to induce a pro-inflammatory phenotype in fibroblasts [35]. Furthermore, while IL-22 is largely thought of a T$_H$17 cell cytokine, they are not the only source: CD8+ T cells, natural killer T cells, and γδ T cells are all able to produce IL-22, and the source of IL-22 likely varies depending on the pathologic condition [22].

In GL261 tumor-bearing mice, we found that, compared to isotype antibody treatment, anti-VEGF therapy resulted in significantly higher tumor levels of IL-22. This suggests
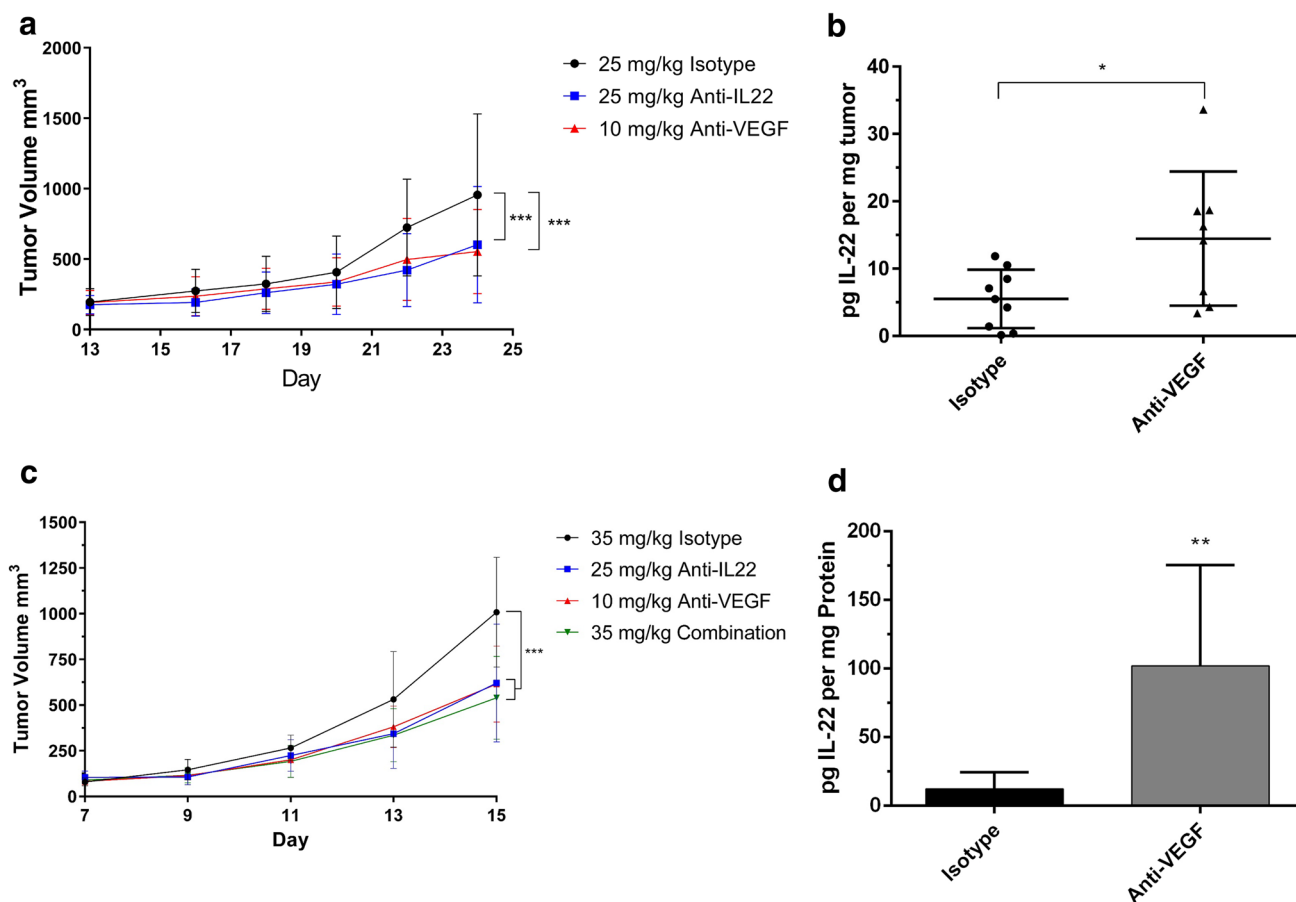
Fig. 7 Effects of anti-IL-22 on GL261 tumor growth. **a** Tumor volume of GL261 tumors implanted in C57BL/6 mice ($n = 9$–10). **b** Intratumoral IL-22 levels in C57BL/6 mice, determined by ELISA ($n = 8$–10). **c** Tumor volume of GL261 tumors implanted in athymic nude mice ($n = 10$). **d** Intratumoral IL-22 levels in athymic nude mice, determined by ELISA ($n = 10$). Error bars indicate standard deviation, $*p < 0.05$, $**p < 0.01$, $***p < 0.001$

that IL-22 may be upregulated in GL261 tumors in vivo as a method of escaping anti-angiogenic pharmacological inhibition. However, as already noted, we were unable to document any additive or synergistic effects from the combination of anti-VEGF with anti-IL-22 antibodies. The reasons for these findings remain unclear, but recent studies emphasize that up-regulation of a potential target does not necessarily predict a combinatorial benefit. For example, in spite of cMet upregulation, the combination of cMet inhibitors with VEGF or EGFR inhibitors so far has failed to result in the anticipated additive benefits in cancer patients, for reasons that remain to be elucidated [36, 37].

Despite the tumor inhibition observed in vivo following anti-IL22 and anti-VEGF therapy, in contrast to the EL4 model, staining for CD31 did not demonstrate a statistically significant difference in blood vessel density for treated GL261 tumor bearing mice. However, the anti-angiogenic effect of a therapy is more complex than simply the density of blood vessels within the tumor [38]. It has been pointed out that although microvessel density is

a useful prognostic marker, it may not be an indicator of anti-angiogenic treatment efficacy, since to a large extent it reflects the metabolic burden of tumor cells [39]. Also, other studies have shown that angiogenesis inhibitors can in some cases paradoxically increase tumor blood flow and oxygenation during the initial few weeks of treatment [40, 41] and furthermore that some benefit of anti-angiogenic therapy may arise from reducing interstitial pressure, without resulting in major reductions in blood vessel density [42]. Alternatively, it is possible that the aforementioned non-angiogenic, protumor mechanisms of IL-22 play a more prominent role in the GL261 model as compared to the EL4 model.

In summary, our work demonstrates that IL-22 can act directly on endothelial cells to stimulate angiogenesis through activation of the ERK and Stat3 pathways. Blockade of IL-22 inhibits tumor growth associated with reduced tumor angiogenesis, potentially providing a rationale for developing anti-IL-22 therapies for cancer treatment.

Materials and methods

Mice

C57BL/6 and Rag1$^{-/-}$ mice at 6–8 weeks were purchased from Jackson Laboratories (Bar Harbor, ME). Female (6–8 weeks) athymic nude mice were bred in the animal facility at University of California San Diego. Animals were housed in pathogen-free conditions and experimental procedures were carried out in accordance with established standards of care and approved protocols from the Animal Care and Use Committee of the University of California, San Diego. Prior to tissue harvest, mice were euthanized by CO_2 inhalation followed by cervical dislocation.

Cell culture

Primary human umbilical vein endothelial cells from pooled donors (HUVEC, Lonza Walkersville Inc., Walkersville, MD, #C2519AS), passage 4–8, were cultured on 0.1% gelatin-coated plates in EGM-2 endothelial cell growth media (Lonza Walkersville Inc., Walkersville, MD, #CC3162). Primary human lung microvascular endothelial cells from single donor (HMVEC, Lonza Walkersville Inc., Walkersville, MD, #CC-2527), passage 3–6, were cultured on 0.1% gelatin coated plates in EGM-2 microvascular cell growth media (Lonza Walkersville Inc., Walkersville, MD, #CC3202). EL4 cells were purchased from ATCC (Manassas, VA, #TIB-39) and maintained in high glucose Dulbecco's modified Eagle's medium (DMEM, Hyclone, Logan, UT, #SH30243.01) supplemented with 10% fetal bovine serum (FBS, Omega Scientific, Inc., Tarzana, CA, #FB-02). The GL261 cell line [43] was a gift from Dr. Santosh Kesari (UCSD) and was maintained in high glucose DMEM supplemented with 10% FBS. Cells were maintained at 37 °C in a humidified atmosphere with 5% CO_2.

Endothelial cell proliferation and survival

For cell proliferation, 10^4 HUVECs or HMVECs suspended in 100 µl EBM-2 (Lonza Walkersville Inc., Walkersville, MD, #CC3156) with 10% FBS were seeded in 12-well plates previously coated with gelatin. Four hours later, recombinant human interleukin-22 (Cell Signaling Tech. Inc., Danvers, MA, #8931SF) at concentrations of 5, 10, 25, 50, or 100 ng/mL resuspended in PBS containing 0.1% BSA (Fischer Scientific, Waltham, MA, #BP1605-100) or PBS with 0.1% BSA (control) was added to cells. HUVECs were incubated for 3 days. HMVECs were cultured for 6 days and on day 3, fresh media with cytokine were added. At the end of the experiments, cell numbers were determined using

the Countess cell counter (Invitrogen, Carlsbad, CA). Fold changes were calculated as the ratios between IL-22-treated and control groups. Statistical testing was performed by one-way ANOVA with post-hoc Dunnett's test for multiple comparisons.

For cell survival, 10^3 HUVECs or HMVECs, suspended in 100 µl EBM-2 with 2% FBS, were seeded in 96-well plates previously coated with gelatin. Four hours later, recombinant human interleukin-22 at concentrations of 5, 10, 25, 50, or 100 ng/mL in PBS containing 0.1% BSA or PBS with 0.1% BSA (control) was added to cells. HUVECs were incubated for 3 days. HMVECs were cultured for 6 days and on day 3, fresh media with cytokine were added. At the end of the experiments, cell survival was determined using the Cell Viability/Cytotoxicity assay (Advanced BioReagents, Hayward, CA, K020), following the manufacturer's instruction. Fold changes were calculated as the ratios between IL-22-treated and control groups. Statistical testing was performed by one-way ANOVA with post-hoc Dunnett's test for multiple comparisons.

Conditioned media preparation and IL-22 ELISA

For measurement of IL-22 concentration in conditioned media, one million EL4 cells in 25 cm^2-flasks were stimulated with 1 ng/mL TGF-β1 (R&D systems, Minneapolis, MN, #7666-MB) and 20 ng/mL IL-6 (Peprotech, Rocky Hill, NJ, #216-16) at the time of plating in high glucose DMEM supplemented with 2% FBS. Cells were cultured with ambient O_2 (normoxia) or with 1% O_2 (hypoxia). After 6 days, media were collected and centrifuged to remove debris. IL-22 concentrations were measured by an ELISA kit (R&D systems, Minneapolis, MN, #M2200), according to the manufacturer's instructions. Statistical analysis was performed by one-way ANOVA with Tukey's test correction for multiple comparisons.

For measurement of tumor IL-22 concentrations, tumor samples were weighed and then homogenized using cell lysis buffer (R&D systems, #895347). Total protein concentrations in tumor lysates were determined by the BCA assay (Thermo Fisher Scientific, Waltham, MA, #23225). IL-22 concentrations were measured by ELISA and normalized to tumor weight or total protein concentrations. Statistical analysis was performed by Welch's t-test.

Western blots

HUVECs or HMVECs were plated and starved in EBM-2 with 2% FBS overnight before recombinant human IL-22 at concentrations of 5, 10, 20, 50, or 100 ng/mL or PBS with 0.1% BSA (control) was added. After 30 min, cells were then lysed with RIPA buffer (Thermo Fisher Scientific, Waltham, MA, #89901) containing 1% phosphatase/protease

inhibitor (Thermo Fisher Scientific, #1861281). The lysate was centrifuged for 30 min at 14,000×g to remove debris, and stored at − 80 °C. Protein concentrations in cell lysates were determine by the BCA assay (Thermo Fisher Scientific, #23225) and equal amounts of protein were loaded to NuPAGE 4–12% Bis-Tris gels (Thermo Fisher Scientific, #NP0321BOX, #NP0323BOX) then transferred onto a nitrocellulose membrane. Membranes were blocked and incubated with primary antibodies [Anti–β–actin (Sigma-Aldrich, St. Louis, MO, #A2228), anti-Phospho-ERK1/2 (Cell Signaling, #4376S), anti-ERK1/2 (Cell Signaling, #4695S), anti-STAT3 (Cell Signaling, #4904S), anti-Phospho-STAT3 (Cell Signaling, #9145S), or anti-IL-22Rα1 (Abcam, Cambridge, MA, #ab5984). Membranes were then incubated with secondary antibodies (GE Healthcare, Pittsburg, PA, #NA931, #NA934) and developed with SuperSignal West Chemiluminescent substrates (Thermo Fisher Scientific, #34580, #34096)]. Western Blot results were quantified by measuring the area of individual bands of phosphorylated and total proteins using Image J. The ratios between phosphorylated and total proteins were calculated for normalization purpose. Statistical analysis was performed by Student's t-test.

Mouse choroidal explant assay

Using pre-cooled pipette tips, 130 µL of reduced growth factor basement membrane extract (BME) (Trevigen, Gaithersburg, MD, #3433-005-R1) was added to each well in a 48-well plate. To avoid evaporation, surrounding wells were filled with PBS. BME was allowed to solidify at 37 °C for 20 min. One peripheral sclerochoroidal wedge, dissected from male C57BL/6J (age P20) mice, was added to the center of each well, as previously described [24, 25]. Care was taken to disrupt the tissue minimally. Each experimental condition was tested from explants from a single eye. The tissue was incubated at 37 °C for 15 min prior to the addition of a top layer of 130 µL BME. After a 30 min incubation period, 500 µL of growth media was added to each well (human endothelial serum free-media (Lonza Walkersville Inc., Walkersville, MD, #CC3156) containing 2% FBS, 50 units/ml penicillin and 50 mg/ml streptomycin), plus varying concentrations of IL-22 or VEGF$_{165}$. Explants were incubated in standard cell culture conditions with 5% CO_2. Fresh media was exchanged at day 2 and day 4. Images were taken on day 6 using an inverted microscope with a 10× objective and acquired using Axiovision LE Rel.4.4 software. Vessel outgrowth was quantified using ImageJ. Data from three experiments were pooled for a total number of 6–10 replicates per condition. Statistical analysis was performed by one-way ANOVA with post-hoc Dunnett's test for multiple comparisons.

Tumor cell viability assays

For IL-22 Stimulation, 1×10^3 GL261 or 2.5×10^3 EL4 cells were seeded onto 96-well plates in high glucose DMEM supplemented with 2% FBS. At the time of seeding, recombinant interleukin-22 resuspended in PBS containing 0.1% BSA was added to cells at concentrations of 5, 10, 25, 50, or 100 ng/mL. 1 µL/mL PBS containing 0.1% BSA was used as a negative control and comparison. Dulbecco's Modified Eagle's Medium with high glucose supplemented and 10% FBS was utilized as a positive control and comparison. After 6 days, cell viability was measured by the Alamar Blue assay (Fisher Scientific, Hampton, NH, #PI88952). Data from three experiments were pooled for a total number of 6–11 replicates per condition. Statistical analysis was performed by one-way ANOVA with Tukey's test correction for multiple comparisons.

To test the effects of anti-IL-22 antibodies, 1×10^3 GL261 or 2.5×10^3 EL4 cells were seeded onto 96-well dishes in high glucose DMEM supplemented with 10% FBS. At the time of seeding, anti-IL-22 (Genentech, South San Francisco, CA, clone 8E11) or isotype control (Bio X-Cell, West Lebanon, NH, #BE0083) antibody was added to EL4 and GL261 cells at concentrations of 0.5, 1, 2.5, 10, 25, or 50 µg/mL. After 6 days, cell viability was measured by the Alamar Blue assay. Data from 3 experiments were pooled for a total number of 5–8 replicates per experimental condition. Statistical analysis was performed by two-way ANOVA with Tukey's test correction for multiple comparisons.

Migration assays

HUVECs or HMVECS (passage 6–8) were cultured and serum-starved as described above. 10,000 cells in 150 µl EBM-2 were added to the upper inserts (8 µm pore size, 24-well) (Falcon, Corning, NY, #62406-198) precoated with 0.1% gelatin. The lower well was filled with 600 µL EBM-2 containing recombinant interleukin-22 resuspended in PBS containing 0.1% BSA was added to cells at concentrations of 5, 10, 25, 50, or 100 ng/mL at the time of plating in EBM-2 media.1 µL/mL PBS containing 0.1% BSA was used as a negative control. 50 ng/mL VEGF$_{165}$ (R&D systems, Minneapolis, MN, #293-VE) was utilized as a positive control. The plates were incubated at 37 °C for 4 h (HUVECs) or 8 h (HMVECs), Cells that migrated across the membrane were fixed with 4% paraformaldehyde (PFA) for 30 min and then stained with crystal violet (Sigma Aldrich, St. Louis, MO, #HT90132-1L) for 30 min at room temperature. Migrated cells in the whole area of the inserts were counted. Data from 4 experiments was pooled for a total number of 8–18 replicates per condition. Statistical analysis was performed by one-way ANOVA with Dunnett's test correction for multiple comparisons.

EL4 in vivo studies

C57BL/6 and Rag1$^{-/-}$ Mice were injected subcutaneously with 1×10^6 cells in a 1:1 mixture of reduced growth factor basement membrane extract (Trevigen, Gaithersburg, MD, #3433-005-R1) and sterile PBS. Treatment was started on day 5 post-tumor cell injection and administered by intraperitoneal injection with 10 mg/kg of anti-VEGF (Genentech, South San Francisco, CA, clone B20.4.1), 6, 12, or 25 mg/kg of anti-IL-22 (Genentech, South San Francisco, CA, clone 8E11), combination of 10 mg/kg anti-VEGF and 25 mg/kg anti-IL-22 or same amounts of isotype control (Bio X-Cell, West Lebanon, NH, #BE0083). Mice were treated every other day throughout the study. Primary tumor volumes were measured by a caliper and calculated using the following formula: $0.5 \times length \times width^2$. Statistical analysis was performed using a mixed-effects model for tumor growth. For comparison of tumor weights, statistical analysis was performed by one-way ANOVA with post-hoc Tukey's test for multiple comparisons.

GL261 in vivo studies

Mice were injected subcutaneously with 1×10^6 cells in a 1:1 mixture of reduced growth factor basement membrane extract and PBS. Treatment began on day 16 for C57BL/6 mice or day 6 for athymic nude mice. Mice were treated *i.p.* with 10 mg/kg of anti-VEGF, 25 mg/kg of anti-IL22, alone or in combination, or same amounts of isotype control (Bio X-Cell) every other day throughout the study. Primary tumor volumes were measured as described above. Statistical analysis was performed using a mixed-effects model.

Flow cytometry analysis

Cells were stained with a PE-conjugated an antibody against IL22Rα1 (R&D Systems, Minneapolis, MN, #FAB2770P) or with an IgG1A isotype control (R&D Systems, Minneapolis, MN, #IC002P) according to the manufacturer's directions and incubated with DAPI (Biolegend, San Diego, CA, #422801) to exclude nonviable cells. Samples were analyzed by BD Fortessa and mean fluorescence intensity was determined by the FlowJo software. Results are from 3 independent experiments with statistical testing by mixed-effects model analysis.

Immunofluorescence staining

Tumor samples were embedded in the Optimum Cutting Temperature compound and frozen. Tumor sections were cut at 10 μm thickness by a Leica CM3050S Cryostat (Leica Biosystems, Buffalo Grove, IL) and fixed in 4% PFA for 15 min at room temperature. Nonspecific binding sites were blocked by incubation in 10% normal goat serum for 1 h at room temperature. Tumor sections were stained with rat anti-mouse CD31 (BD Biosciences, Franklin Lakes, NJ, #550274) at 1:200 overnight at 4 °C, followed by one hour incubation with 1:400 of Alexa Fluor 488 conjugated goat anti-rat IgG (Biolegend, San Diego, CA, #405418) at room temperature. Slides were counterstained with Hoechst 33342, (Thermo Fisher Scientific, Waltham, MA, #H3570) and mounted in Prolong Gold Antifade Mountant (Thermo Fisher Scientific, Waltham, MA, #P36930). Immunofluorescence images were collected on a Keyence BZ-X700 microscope. Statistical analysis was performed by one-way ANOVA with Tukey's test correction for multiple comparisons.

Image analysis

All image analysis was done using ImageJ (National Institute of Health, Bethesda, MD). Cell counting was done manually using the cell counter function.

Statistical analysis

All experiments were performed at least three times. Statistical parameters, including the value of n, are indicated in the figure legends. All statistical analysis was conducted in Graphpad Prism 8 software (https://www.graphpad.com). One-way ANOVA, two-way ANOVA, mixed effects model, and unpaired t-tests were used as statistical tests. All statistical tests used post-hoc analysis when appropriate to account for multiple comparisons. The department of Biostatistics and Bioinformatics at Moores UCSD Cancer Center was consulted to ensure that the appropriate statistical test was utilized. Data are considered significant when $p < 0.05$. Significant p values are represented in the figures as follows: $***p < 0.001$, $**p < 0.01$, $*p < 0.05$.

References

1. Ferrara N, Adamis AP (2016) Ten years of anti-vascular endothelial growth factor therapy. Nat Rev Drug Discov 15(6):385–403
2. Brauer MJ, Zhuang G, Schmidt M, Yao J, Wu X, Kaminker JS, Jurinka SS, Kolumam G, Chung AS, Jubb A, Modrusan Z, Ozawa T, James CD, Phillips H, Haley B, Tam RN, Clermont AC, Cheng JH, Yang SX, Swain SM, Chen D, Scherer SJ, Koeppen H, Yeh RF, Yue P, Stephan JP, Hegde P, Ferrara N, Singh M, Bais C (2013) Identification and analysis of in vivo VEGF downstream

markers link VEGF pathway activity with efficacy of anti-VEGF therapies. Clin Cancer Res 19(13):3681–3692

3. Landskron G, De la Fuente M, Thuwajit P, Thuwajit C, Hermoso MA (2014) Chronic inflammation and cytokines in the tumor microenvironment. J Immunol Res. https://doi.org/10.1155/2014/149185

4. Motz GT, Santoro SP, Wang LP, Garrabrant T, Lastra RR, Hagemann IS, Lal P, Feldman MD, Benencia F, Coukos G (2014) Tumor endothelium FasL establishes a selective immune barrier promoting tolerance in tumors. Nat Med 20(6):607–615

5. Quail DF, Bowman RL, Akkari L, Quick ML, Schuhmacher AJ, Huse JT, Holland EC, Sutton JC, Joyce JA (2016) The tumor microenvironment underlies acquired resistance to CSF-1R inhibition in gliomas. Science 352(6288):aad3018. https://doi.org/10.1126/science.aad3018

6. Negri L, Ferrara N (2018) The prokineticins: neuromodulators and mediators of inflammation and myeloid cell-dependent angiogenesis. Physiol Rev 98(2):1055–1082

7. Pietras K, Pahler J, Bergers G, Hanahan D (2008) Functions of paracrine PDGF signaling in the proangiogenic tumor stroma revealed by pharmacological targeting. PLoS Med 5(1):e19

8. Crawford Y, Kasman I, Yu L, Zhong C, Wu X, Modrusan Z, Kaminker J, Ferrara N (2009) PDGF-C mediates the angiogenic and tumorigenic properties of fibroblasts associated with tumors refractory to anti-VEGF treatment. Cancer Cell 15:21–34

9. Beenken A, Mohammadi M (2009) The FGF family: biology, pathophysiology and therapy. Nat Rev Drug Discov 8(3):235–253

10. Ellis LM, Hicklin DJ (2008) VEGF-targeted therapy: mechanisms of anti-tumour activity. Nat Rev Cancer 8(8):579–591

11. Chung AS, Wu X, Zhuang G, Ngu H, Kasman I, Zhang J, Vernes JM, Jiang Z, Meng YG, Peale FV, Ouyang W, Ferrara N (2013) An interleukin-17-mediated paracrine network promotes tumor resistance to anti-angiogenic therapy. Nat Med 19:1114–1123

12. Coffelt SB, Kersten K, Doornebal CW, Weiden J, Vrijland K, Hau CS, Verstegen NJ, Ciampricotti M, Hawinkels LJ, Jonkers J, de Visser KE (2015) IL-17-producing gammadelta T cells and neutrophils conspire to promote breast cancer metastasis. Nature 522(7556):345–348

13. Saharinen P, Eklund L, Alitalo K (2017) Therapeutic targeting of the angiopoietin-TIE pathway. Nat Rev Drug Discov 16(9):635–661

14. Liang W, Ferrara N (2016) The complex role of neutrophils in tumor angiogenesis and metastasis. Cancer Immunol Res 4(2):83–91. https://doi.org/10.1158/2326-6066

15. Fridman WH, Pages F, Sautes-Fridman C, Galon J (2012) The immune contexture in human tumours: impact on clinical outcome. Nat Rev Cancer 12(4):298–306

16. Basu R, Hatton RD, Weaver CT (2013) The Th17 family: flexibility follows function. Immunol Rev 252(1):89–103

17. Su X, Ye J, Hsueh EC, Zhang Y, Hoft DF, Peng G (2010) Tumor microenvironments direct the recruitment and expansion of human Th17 cells. J Immunol 184(3):1630–1641

18. Zheng Y, Danilenko DM, Valdez P, Kasman I, Eastham-Anderson J, Wu J, Ouyang W (2007) Interleukin-22, a T(H)17 cytokine, mediates IL-23-induced dermal inflammation and acanthosis. Nature 445(7128):648–651

19. Rutz S, Eidenschenk C, Ouyang W (2013) IL-22, not simply a Th17 cytokine. Immunol Rev 252(1):116–132

20. Wu T, Cui L, Liang Z, Liu C, Liu Y, Li J (2013) Elevated serum IL-22 levels correlate with chemoresistant condition of colorectal cancer. Clin Immunol 147(1):38–39

21. Kirchberger S, Royston DJ, Boulard O, Thornton E, Franchini F, Szabady RL, Harrison O, Powrie F (2013) Innate lymphoid cells sustain colon cancer through production of interleukin-22 in a mouse model. J Exp Med 210(5):917–931

22. Sabat R, Ouyang W, Wolk K (2014) Therapeutic opportunities of the IL-22-IL-22R1 system. Nat Rev Drug Discov 13(1):21–38

23. Nowak-Sliwinska P, Alitalo K, Allen E, Anisimov A, Aplin AC, Auerbach R, Augustin HG, Bates DO, van Beijnum JR, Bender RHF, Bergers G, Bikfalvi A, Bischoff J, Bock BC, Brooks PC, Bussolino F, Cakir B, Carmeliet P, Castranova D, Cimpean AM, Cleaver O, Coukos G, Davis GE, De Palma M, Dimberg A, Dings RPM, Djonov V, Dudley AC, Dufton NP, Fendt SM, Ferrara N, Fruttiger M, Fukumura D, Ghesquiere B, Gong Y, Griffin RJ, Harris AL, Hughes CCW, Hultgren NW, Iruela-Arispe ML, Irving M, Jain RK, Kalluri R, Kalucka J, Kerbel RS, Kitajewski J, Klaassen I, Kleinmann HK, Koolwijk P, Kuczynski E, Kwak BR, Marien K, Melero-Martin JM, Munn LL, Nicosia RF, Noel A, Nurro J, Olsson AK, Petrova TV, Pietras K, Pili R, Pollard JW, Post MJ, Quax PHA, Rabinovich GA, Raica M, Randi AM, Ribatti D, Ruegg C, Schlingemann RO, Schulte-Merker S, Smith LEH, Song JW, Stacker SA, Stalin J, Stratman AN, Van de Velde VM, van Hinsbergh VWM, Vermeulen PB, Waltenberger J, Weinstein BM, Xin H, Yetkin-Arik B, Yla-Herttuala S, Yoder MC, Griffioen AW (2018) Consensus guidelines for the use and interpretation of angiogenesis assays. Angiogenesis. https://doi.org/10.1007/s10456-018-9613-x

24. Xin H, Zhong C, Nudleman E, Ferrara N (2016) Evidence for pro-angiogenic functions of VEGF-Ax. Cell 167(1):275–284 e276

25. Shao Z, Friedlander M, Hurst CG, Cui Z, Pei DT, Evans LP, Juan AM, Tahiri H, Duhamel F, Chen J, Sapieha P, Chemtob S, Joyal JS, Smith LE (2013) Choroid sprouting assay: an ex vivo model of microvascular angiogenesis. PLoS ONE 8(7):e69552

26. Shojaei F, Wu X, Malik AK, Zhong C, Baldwin ME, Schanz S, Fuh G, Gerber HP, Ferrara N (2007) Tumor refractoriness to anti-VEGF treatment is mediated by CD11b + Gr1 + myeloid cells. Nat Biotechnol 25(8):911–920

27. Tan AH, Lam KP (2010) Pharmacologic inhibition of MEK-ERK signaling enhances Th17 differentiation. J Immunol 184(4):1849–1857

28. Dumoutier L, Van Roost E, Colau D, Renauld JC (2000) Human interleukin-10-related T cell-derived inducible factor: molecular cloning and functional characterization as an hepatocyte-stimulating factor. Proc Natl Acad Sci U S A 97(18):10144–10149

29. He X, Li H, Chen Y, Chen A, Shan K, Chen J, Zhao H, Zhang X, Cai T (2016) The Effects of IL-22 on the Inflammatory Mediator Production, Proliferation, and Barrier Function of HUVECs. Inflammation 39(3):1099–1107

30. Wu Z, Hu Z, Cai X, Ren W, Dai F, Liu H, Chang J, Li B (2017) Interleukin 22 attenuated angiotensin II induced acute lung injury through inhibiting the apoptosis of pulmonary microvascular endothelial cells. Sci Rep 7(1):2210

31. Shang WQ, Yu JJ, Zhu L, Zhou WJ, Chang KK, Wang Q, Li MQ (2015) Blocking IL-22, a potential treatment strategy for adenomyosis by inhibiting crosstalk between vascular endothelial and endometrial stromal cells. Am J Transl Res 7(10):1782–1797

32. Lejeune D, Dumoutier L, Constantinescu S, Kruijer W, Schuringa JJ, Renauld JC (2002) Interleukin-22 (IL-22) activates the JAK/STAT, ERK, JNK, and p38 MAP kinase pathways in a rat hepatoma cell line. Pathways that are shared with and distinct from IL-10. J Biol Chem 277(37):33676–33682

33. Wolk K, Kunz S, Witte E, Friedrich M, Asadullah K, Sabat R (2004) IL-22 increases the innate immunity of tissues. Immunity 21(2):241–254

34. Kohler T, Reizis B, Johnson RS, Weighardt H, Forster I (2012) Influence of hypoxia-inducible factor 1alpha on dendritic cell differentiation and migration. Eur J Immunol 42(5):1226–1236

35. Brembilla NC, Dufour AM, Alvarez M, Hugues S, Montanari E, Truchetet ME, Lonati P, Fontao L, Gabrielli A, Vettori S, Valentini G, Boehncke WH, Meroni P, Chizzolini C (2016) IL-22

capacitates dermal fibroblast responses to TNF in scleroderma. Ann Rheum Dis 75(9):1697–1705

36. Bendell JC, Hochster H, Hart LL, Firdaus I, Mace JR, McFarlane JJ, Kozloff M, Catenacci D, Hsu JJ, Hack SP, Shames DS, Phan SC, Koeppen H, Cohn AL (2017) A phase II randomized trial (GO27827) of first-line FOLFOX plus bevacizumab with or without the met inhibitor onartuzumab in patients with metastatic colorectal cancer. Oncologist 22(3):264–271

37. Spigel DR, Edelman MJ, O'Byrne K, Paz-Ares L, Mocci S, Phan S, Shames DS, Smith D, Yu W, Paton VE, Mok T (2016) Results from the phase III randomized trial of onartuzumab plus erlotinib versus erlotinib in previously treated stage IIIB or IV non-small-cell lung cancer: METLung. J Clin Oncol 31(32):4105–4114

38. Folkman J (2007) Angiogenesis: an organizing principle for drug discovery? Nat Rev Drug Discov 6(4):273–286

39. Hlatky L, Hahnfeldt P, Folkman J (2002) Clinical application of antiangiogenic therapy: microvessel density, what it does and doesn't tell us. J Natl Cancer Inst 94(12):883–893

40. Teicher BA, Dupuis N, Kusomoto T (1994) Antiangiogenic agents can increase tumor oxygenation and response to radiation therapy. Radiat Oncol Investig 2(6):269–276

41. Teicher BA, Holden SA, Ara G, Dupuis NP, Liu F, Yuan J, Ikebe M, Kakeji Y (1995) Influence of an anti-angiogenic treatment on 9L gliosarcoma: oxygenation and response to cytotoxic therapy. Int J Cancer 61(5):732–737

42. Jain RK (2001) Normalizing tumor vasculature with anti-angiogenic therapy: a new paradigm for combination therapy. Nat Med 7(9):987–989

43. Jacobs VL, Valdes PA, Hickey WF, De Leo JA (2011) Current review of in vivo GBM rodent models: emphasis on the CNS-1 tumour model. ASN Neuro 3(3):e00063. https://doi.org/10.1042/AN20110014